Dalton Transactions

PAPER

View Article Online
View Journal | View Issue

CrossMark click for updates

Cite this: *Dalton Trans.*, 2016, **45**, 6282

Synthesis and reactivity of fluorenyl-tethered N-heterocyclic stannylenes†

Marta Roselló-Merino and Stephen M. Mansell*

Received 16th October 2015,
Accepted 19th December 2015

DOI: 10.1039/c5dt04060d

www.rsc.org/dalton

A fluorenyl (Fl) tethered diamine was synthesised by nucleophilic substitution of (bromoethyl)fluorene with a diisopropylphenyl (Dipp) substituted diamine to give $FlC_2H_4N(H)C_2H_4N(H)Dipp$ (**1a**) in good yield (85%). Lithiation of **1a** with *n*-BuLi proceeded with coordination of the Li cation to the aromatic fluorenide ring (**2**), and with subsequent equivalents of *n*-BuLi, the secondary amines were then sequentially deprotonated. A fluorenyl-tethered N-heterocyclic stannylene (NHSn) was synthesised from the reaction of **1a** with SnN''_2 {N'' = $N(SiMe_3)_2$} as a neutral dimeric species (**5**), and this was deprotonated with LiN'' to give the corresponding dianionic fluorenide-tethered NHSn (**6**). Reactions of [{Rh(cod)(μ-Cl)}$_2$] with the mono-deprotonated ligand **2** led to the formation of a mixed-donor amide–amine Rh(I) compound (**7**), whereas reactions with the anionic NHSn **6** led to a Rh–fluorenyl complex of low stability with an uncoordinated pendent NHSn arm, which X-ray crystallography showed to be dimeric in the solid state.

Introduction

Tethered ligands are interesting candidates for designing new generations of homogeneous catalysts as they allow the combination of different ligand classes into one flexible chelating ligand.[1] Alternatively, they can be designed to facilitate the immobilisation of a homogeneous catalyst on a solid support.[2] Due to the exceptional properties of the cyclopentadienyl ligand in transition metal chemistry, tethered ligands typically consist of an anionic cyclopentadienyl moiety, or a fused analogue such as indenyl or fluorenyl, attached *via* a hydrocarbon linker to a second donor group (Fig. 1, **A**) which can be anionic or neutral, hard or soft according to Pearson's HSAB classification.[3,4] Other anionic anchor groups have also been explored such as alkoxide or amide, particularly for tethered N-heterocyclic carbenes (NHCs).[5] The combination of an anionic and strongly binding anchor with the alternative properties provided by the tethered donor can give rise to hemilability,[6] an area of increasing interest in catalysis where stabilisation of some intermediates in a catalytic cycle may be required without permanently reducing the catalytic effectiveness of the complex.[7] Tethered ligands can also promote the formation of bimetallic complexes[8] or 1,2 reactions across the metal–ligand bond.[9,10]

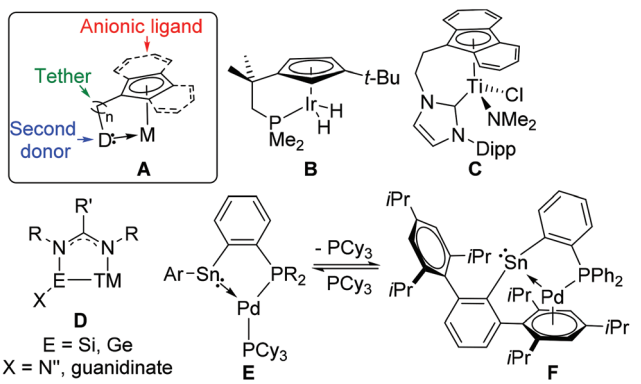

Fig. 1 Examples of transition metal complexes of tethered ligands.

Research into tethered Cp compounds has been explored in particular depth for the group 4 metals owing to continued interest in metallocene-based polymerisation catalysts, and the 'constrained geometry catalyst' family, bearing an amido tether pendent to a Cp group, has been shown to produce poly(alkenes) with unique material properties.[11,12] Focusing on the tethered donor, anionic oxygen donors[4] are suitable for binding to electropositive metals, but of great interest are soft donor atoms such as P, S and As due to the contrast with the Cp unit,[3] and C–H activation reactivity has been observed for group 9 phosphine-tethered Cp complexes under UV-irradiation.[13,14] In the C_1 symmetric Ir complex **B**, C–H acti-

Institute of Chemical Sciences, Heriot-Watt University, Edinburgh, EH14 4AS, UK. E-mail: s.mansell@hw.ac.uk

†Electronic supplementary information (ESI) available: Additional synthetic details for $^tBuN(H)C_2H_4NH_2$, **1b**, **1c** and **1d**, NMR spectra for all the compounds and additional crystallographic information including the crystal structures of **1a** (in $P\bar{1}$), **1b** and **1b**·2HCl. CCDC 1424295–1424301, 1431076 and 1441450. For ESI and crystallographic data in CIF or other electronic format see DOI: 10.1039/c5dt04060d. Additional research data supporting this publication are available from Heriot-Watt University's research data repository at DOI: 10.17861/ac16915b-851c-4007-8fe3-38a13d6c97d1

vation of cyclohexane occurred with the formation of only one diastereomer due to a steric clash between cyclohexyl and *tert*-butyl substituents in the product, demonstrating a decisive role for the ligand in improving product selectivity.[14] Unsaturated NHC-tethered Cp ligands represent a relatively new field of research,[15,16] but a growing number of ligands and complexes have been reported (*e.g.* **C**)[17] which have shown promise in catalysis.[18–22]

The study of heavier group 14 carbene analogues, pioneered by Lappert and co-workers,[23,24] is of current interest[25,26] due to their distinctive donor properties, including less directional σ-donation through a donor orbital of high s-character and π-accepting behaviour.[27] Although the unsaturated analogues of N-heterocyclic stannylenes (NHSns) were found to be thermally unstable,[28,29] saturated[30] and benzannulated[31] NHSns are amenable to coordination and reactivity studies, and demonstrated very different behaviour compared to NHCs, for example, in their ability to bridge metal centres.[32] Bidentate bis(benzannulated-NHSns) linked by hydrocarbon spacers allow chelation of a metal by two Sn centres,[33–35] and a pincer ligand formed from two benzannulated NHSns attached to a pyridine backbone has also been characterised.[36] This concept has also been applied to Si(II) using amidinate supporting ligands with a pyridine backbone.[37]

Tethering a stannylene unit to another donor with contrasting properties is still relatively unexplored. Benzannulated NHSns with neutral methoxy- and dimethylamino-substituted tethers have only demonstrated intramolecular coordination of the tethers to the Sn centres.[34,38] Pyridine-annulated NHSns, which cannot function as chelating ligands to transition metals,[39] have revealed interesting self-assembly into a highly stable tetramer.[40] Guanidinate[41] and amidinate[27,42] ligands have shown unusual behaviour as supporting ligands for Si(II) and Ge(II) (E) as the normal κ^2-chelating binding mode can change to a bridging mode between E and a transition metal acting as a tether to the E–TM interaction (**D**). A recent report has demonstrated that low valent Sn can function as either a donor (**E**) or acceptor (**F**) to Pd as part of a phosphine–stannylene chelate highlighting the unique behavior of Sn(II) compared to lighter analogues.[43] In the context of the anionic tethered ligands described below, recent work on protic NHSns demonstrated deprotonation of a residual N–H with NaH to give an anionic complex.[44,45] In looking to exploit new bimetallic complexes for CH activation,[46] and recognizing that tin has an expanding role in heterobimetallic catalysis,[47] the development of tethered NHSn ligands was targeted for developing new cooperative reactivity.

Results and discussion

Ligand precursor synthesis

Due to the difficulties associated with isomerisation of substituted tetramethylcyclopentadienyl ligands leading to exocyclic C=C bonds,[48] tethered fluorenyl (Fl) ligands were instead selected (**1a**, Scheme 1). The sterically encumbered di-

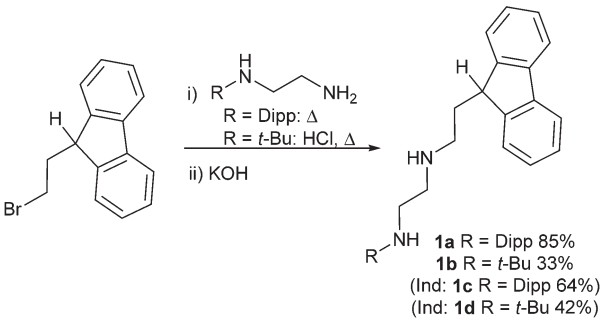

Scheme 1 Synthesis of ligand precursors (Dipp = 2,6-*i*-$Pr_2C_6H_3$, Ind = indenyl analogue).

isopropylphenyl (Dipp) substituent was chosen to facilitate the stabilisation of the corresponding NHSns, and C_2-linkers for the diamine and the tethered fluorene were chosen to avoid ring strain in the corresponding chelate complexes. Indenyl and *tert*-butyl derivatives were also synthesised (**1b**, **1c**, **1d**; see ESI† for details), but were not the focus of subsequent reactivity studies due to the lower yields and more difficult purification of the ligand precursors, particularly for the *tert*-butyl derivatives.

Reactions of the monolithiated diamines $RN(H)C_2H_4N(H)Li$ with (bromoethyl)fluorene quantitatively formed the corresponding spirocycle,[49] and reactions using the free diamines in organic solvent were both slow and unselective. Careful optimisation of the reaction conditions was required to avoid formation of this by-product and also suppress the formation of disubstituted products formed from two equivalents of (bromoethyl)fluorene reacting with the diamine. For R = Dipp, good results were obtained using neat conditions with an excess of diamine, and column chromatography furnished the pure product in good yield (**1a**, 85%). For R = *t*-Bu, additional HCl was required to inhibit the formation of the spirocycle, and the best results were obtained when using a 1 : 2 HCl : diamine ratio and heating the reagents at 100 °C for 1–3 hours (see ESI†). ^{1}H and ^{13}C NMR spectroscopy and elemental analysis were used for characterisation. For **1a**, fast rotation around the N–Dipp bond was observed, as shown by the presence of only one doublet and one septet resonance for the isopropyl groups, and the characteristic resonance of the 9-H in the Fl moiety was observed as a triplet at *ca.* 4 ppm due to coupling to a CH_2 in the ethyl linker. The CH_2 groups in the ethyl linkers were observed between 2 and 3 ppm as multiplets due to second order effects. Single crystals of **1a** crystallised from saturated *n*-hexane solutions upon cooling to −20 °C in the space group $P\bar{1}$, or as a polymorph in $P2_1/c$ after slow evaporation at room temperature. Identical molecular structures were observed in each case with a long intramolecular hydrogen bond between H2 and N1 (both N–H hydrogen atoms were located in the Fourier difference map and their positions refined; Fig. 2). The packing differed between the two polymorphs as although there were no interactions involving H1, short contacts between N2 and H4 (a hydrogen atom on the

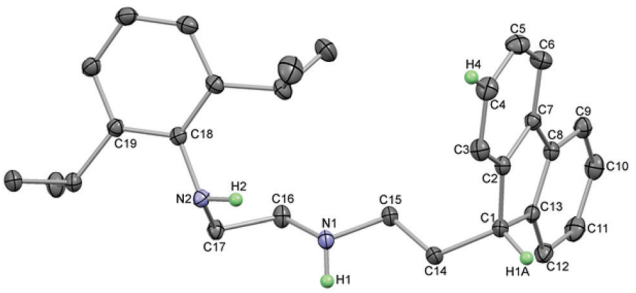

Fig. 2 Thermal ellipsoid plot of the molecular structure of **1a** (50% probability). The positions of only the relevant hydrogen atoms are shown with the rest omitted for clarity. Selected bond distances (Å) and angles (°) for **1a** ($P\bar{1}$): C1–C2 1.526(1), C1–C13 1.528(1), C1–C14 1.546(1), C2–C7 1.416(1), C7–C8 1.482(1), C8–C13 1.415 (1); Σ (angles at C1) 330.9.

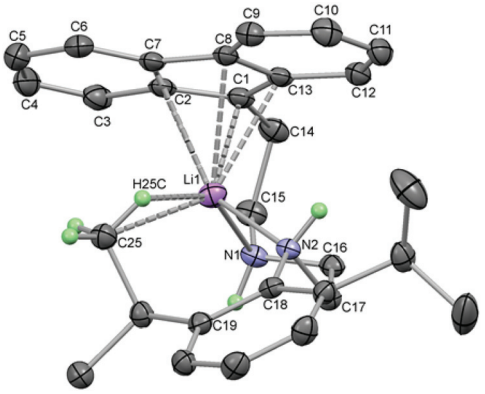

Fig. 3 Thermal ellipsoid plot of the molecular structure of **2** (50% probability). All H atoms except those attached to the nitrogen atoms and C25 have been removed for clarity. Selected bond distances (Å) and angles (°) for **2**: Li1–N1 2.075(2), Li1–N2 2.109(2), Li1–C1 2.289(2), Li1–C2 2.404(2), Li1–C7 2.643(2), Li1–C8 2.658(2), Li1–C13 2.450(2), Li1–C25 2.660, C1–C2 1.436(2), C1–C13 1.440(2), C1–C14 1.519(2), C2–C7 1.456(2), C7–C8 1.453(2), C8–C13 1.465(2); Σ (angles at C1) 359.8.

fluorene ring) formed pairs of molecules in **1a** ($P\bar{1}$), whereas the equivalent interaction was between adjacent molecules in **1a** ($P2_1/n$) forming ribbons (see ESI† for details). The molecular structure of **1a** possesses a tetrahedral carbon centre in the fluorenyl ring with a hydrogen atom present (C1), and the bond lengths and angles are unexceptional.

These reactions represent a simple route into diamine-tethered fluorenyl ligand precursors which feature two N donors, both of which are additionally secondary amines capable of undergoing deprotonation. This introduces much greater ligand versatility compared to conventional (dialkylamino) ethyl tethers.[1,8,50,51]

Lithiation chemistry

With three relatively acidic hydrogen atoms, it was important to establish the sequence of deprotonation for the fluorenyl and amine groups, as well as establish the structures of these anionic species, in order to verify their use as ligand precursors. This was investigated by sequential lithiation of **1a** using one, two and three equivalents of *n*-BuLi (Scheme 2). Addition of *n*-BuLi to a benzene solution of **1a** formed an orange solution. Single crystals suitable for X-ray diffraction grew at room temperature over a period of several days and the molecular structure of **2** was determined (Fig. 3). As expected on pK_a grounds,[52,53] the fluorene 9C atom has been deprotonated with the lithium cation binding to five C atoms in the fluorenide anion in an interaction best described as an asymmetric η^5 coordination mode (Li1–C1 2.289(2), Li1–C2 2.404(2), Li1–C13 2.450(2), Li1–C7 2.643(2), Li1–C8 2.658(2) Å). The ligand has folded so that the two N atoms can function as neutral amine donors to the Lewis acidic Li cation (Li1–N1 2.075(2), Li1–N2 2.109(2) Å), definitively established by location and refinement of the N–H hydrogen atoms. The fourth coordination site of the lithium cation appears to be taken up with an interaction to a methyl C–H bond (Li1–C25 2.660, Li1–H25C 2.183 Å) to give the preferential pseudo-tetrahedral coordination at the Li cation. These distances are longer than the electrostatic interactions observed in the *n*-BuLi hexamer (av. Li–C_β 2.287, Li–H 2.04(2) Å) and the *t*-BuLi tetramer (av. Li–C_β 2.374 Å),[54] but the geometry of the interaction could be an indication of its potential to influence the structure of the complex. For comparison, the structure of $[Li(FlC_2H_4NMe_2)(thf)_2]$ showed the Li cation η^2-bound to the fluorenide (Li–C 2.386(10) and 2.659(10) Å) with pseudo-tetrahedral geometry established by coordination of the NMe_2 tether and two molecules of thf.[51] The energetics favouring specific Fl–Li geometries are apparently subtle as the same compound crystallised from Et_2O with almost identical η^5-Fl distances compared to **2** (Li–C 2.235(5)–2.684(6) Å), but with only one molecule of Et_2O bound to the Li, in addition to the NMe_2 tether, leaving the Li cation in a non-tetrahedral environment.[51] Other Li salts of tethered fluorenide compounds have

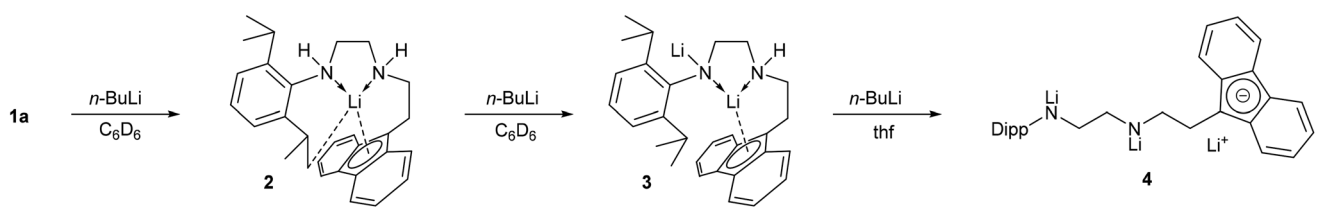

Scheme 2 Lithiation studies of **1a** (Dipp = 2,6-*i*-$Pr_2C_6H_3$).

displayed η^1-,[55] η^2-[56,57] and η^5-interactions[55] highlighting the flexibility of coordination geometries with the fluorenide group.[58]

^{7}Li NMR spectroscopy of **2** in C_6D_6 revealed one resonance at −5.7 ppm, a very distinctive chemical shift indicative of an interaction with an aromatic ring current. Studies on LiFl with a number of donors have established that values of *ca.* −7 ppm represent symmetrical coordination to the 5-membered ring,[59] whereas the solid state NMR shift of $[LiFl(Et_2O)_2]$ (−5.6 ppm),[59] together with asymmetry in the ^{13}C NMR spectra, represent an asymmetric interaction as observed in crystal structures of $[LiFl(Et_2O)_n]$, either η^3 (n = 1)[57] or η^2 (n = 2).[60] This suggests that the asymmetric coordination of **2** is likely to be preserved in non-coordinating solvents. ^{1}H NMR spectroscopy of **2** revealed broad signals at room temperature so a variable temperature NMR study was carried out. Heating to 60 °C caused the signals to sharpen and a symmetric structure was evident without a characteristic triplet for the 9-H atom. Cooling to −50 °C caused uninterpretable broadening of the low frequency signals, but decoalescence of the Fl resonances was observed due to a reduction in symmetry for the complex. Although this dynamic process could not be definitively assigned, the low temperature asymmetric structure is in agreement with the molecular structure observed in the solid state. Addition of thf to this sample produced a sharp set of resonances at room temperature assignable to the complex (see ESI†), although the ^{7}Li NMR resonance at −2.7 ppm indicates that thf has changed the Li–Fl coordination geometry. Addition of a second equivalent of *n*-BuLi to benzene solutions of **2** deprotonated the compound for a second time and ^{7}Li NMR spectroscopy now revealed two resonances, one at −5.7 ppm from identical coordination to the fluorenide ring as seen in **2**, and the other at higher frequency (−2.5 ppm) from deprotonation at another site without close interaction to the Fl ring system. Exchange between these positions must be slower than the NMR timescale. ^{1}H NMR spectroscopy of **3** revealed sharp resonances at room temperature with resonances integrating to one for the individual fluorenide H atoms and only one N–H resonance.

Using NOESY, no through-space correlations were detected between the N–H and the isopropyl groups of the Dipp ligand, with correlations instead observed between the N–H and two adjacent methylene groups supporting the formulation of **3** as deprotonated at the more acidic site. Addition of a third equivalent of *n*-BuLi had to be performed in thf to solubilise the product which displayed only one ^{7}Li NMR resonance at 0.1 ppm, indicating solvent separated ion pairs with $[Li(thf)_4]^+$ cations.[61] A simple set of ^{1}H NMR resonances indicated a symmetric or averaged structure in solution. These results indicate that the site of lowest pK_a (at the fluorenyl) is deprotonated first resulting in coordination of the lithium cation to the fluorenyl ring with two neutral amine donors and an interaction with a C–H bond fulfilling the rest of the coordination sphere. A second and third site of the ligand can also be deprotonated with the same fluorenyl coordination largely retained for **3**, but poor solubility meant that trilithiated **4** required a coordinating solvent for NMR analysis, which breaks up the Li–Fl interactions.

Stannylene formation

Syntheses of tin(II) amides are usually carried out from the reaction of lithium amides with $SnCl_2$, or transamination using $[Sn\{N(SiMe_3)_2\}_2]$ (SnN''_2). The trilithiated ligand precursor **4** was reacted with $SnCl_2$ in OEt_2 in an attempt to form a fluorenide substituted NHSn, but multinuclear NMR spectroscopy revealed that the reaction was not selective. Transamination of SnN''_2 with **1a** in non-coordinating solvents rapidly produced insoluble white precipitate. However, using d^8-thf as a coordinating solvent under dilute conditions (*ca.* 10 mg per cm^3) allowed analysis of the homogeneous reaction mixture (Scheme 3). ^{1}H NMR spectroscopy in d^8-thf revealed the formation of two equivalents of $HN(SiMe_3)_2$ along with

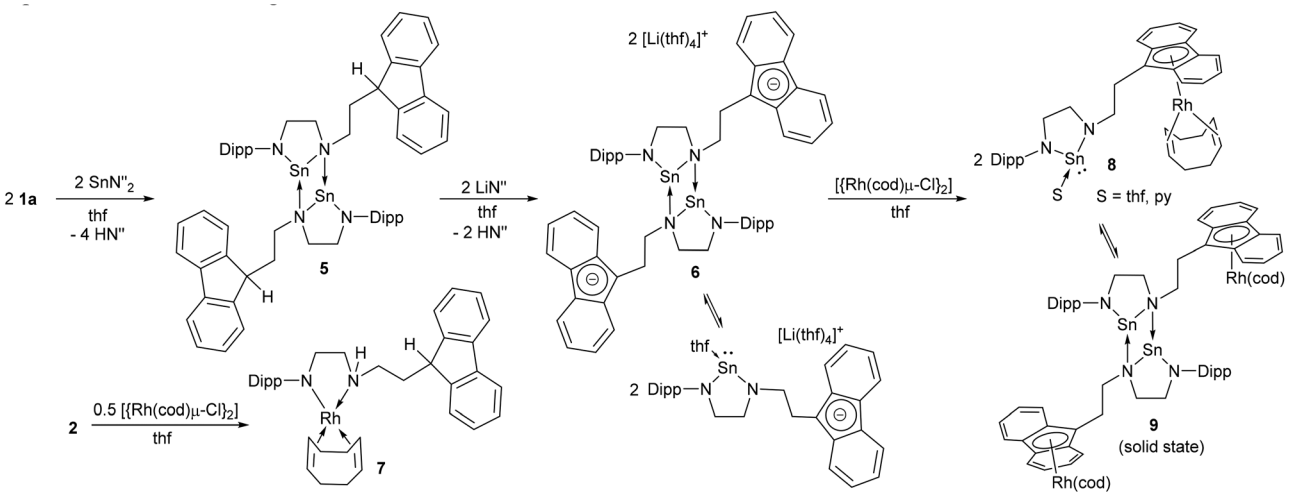

Scheme 3 Synthesis of N-heterocyclic stannylenes and Rh complexes (N'' = $N(SiMe_3)_2$, cod = 1,5-cyclooctadiene).

resonances for a new species with a characteristic triplet at 4 ppm which revealed that the fluorenyl group was intact. ^{119}Sn NMR spectroscopy showed a sharp resonance at +67 ppm which is at much lower frequency compared to previously characterised monomeric, 2-coordinate NHSns (*e.g.* +366 ppm for [Sn{N(Dipp)CH$_2$}$_2$]).[30] This region is characteristic of 3-coordinate NHSns which are dimeric through dative N–Sn bonds (*cf.* + 57 ppm for a dimeric NHSn)[44] or from additional dative bonds from amine tethers (*cf.* +49 to +52 ppm for NHSns with (CH$_2$)$_n$NMe$_2$ tethers).[31]

These data, together with the poor thf solubility of **5**, indicate that this NHSn is likely to be dimeric in solution. Deprotonation of the Fl–H was readily achieved with LiN″ in thf forming the dianionic species **6** which is more soluble than **5** in coordinating solvents. ^{7}Li NMR spectroscopy showed the formation of solvent-separated ion pairs with [Li(thf)$_4$]$^+$ cations (−0.8 ppm), and ^{1}H NMR spectroscopy of **6** in d^8-thf or d^5-pyridine revealed broad resonances indicating more complicated solution behaviour than was seen for **5**. In order to probe this further, a variable temperature NMR study in d^8-thf was carried out. Upon cooling the resonances sharpened and a set of major and minor resonances were observed. For the major set, the broad signals for the *i*-Pr methyl groups separated into four doublets at 0 °C with two resonances coincident (unambiguously established by cooling to −40 °C which caused a slight difference in their chemical shifts). The high frequency region at low temperature showed four resonances each integrating to two H-atoms for the fluorenide group indicating the presence of symmetry at −40 °C, along with a set of minor resonances of low intensity as well. Heating the compound to 55 °C led towards coalescence of the ^{i}Pr Me resonances into one signal before onset of thermal decomposition was identified. This was confirmed by heating a sample of **6** in d^8-toluene which revealed complete decomposition to a new green product at 80 °C which has not been identified (see ESI† for VT NMR study). Decomposition was also observed for **6** in the solid state when heated to 106–111 °C emphasising the relatively low thermal stability of **6**. ^{119}Sn NMR spectroscopy is a useful tool for assessing the coordination number of tin atoms as well as the potential coordination of donor solvents.[62,63] Whereas changing the concentration of **6** in d^8-thf solution made only minor changes to the broad ^{1}H NMR spectra at room temperature, ^{119}Sn NMR spectroscopy revealed a single resonance at high concentration (+53 ppm) but two resonances at low concentration (+224 and +54 ppm). This indicates a concentration dependent monomer – dimer equilibrium is likely to be present, as was inferred by the variable temperature ^{1}H NMR study. In literature studies, the ^{119}Sn NMR resonance for [Sn{N(SiMe$_3$)$_2$}$_2$] reduced from 767 ppm to 602 ppm upon coordination of thf,[62] and a benzannualted stannylene with *N*-Me substituents revealed a similar shift to lower frequency from 222 ppm to 107 ppm upon dissolution in d^8-thf.[38] Typical ^{119}Sn NMR chemical shifts for saturated NHSns are around 360 ppm (*e.g.* 366 ppm for [Sn{N(Dipp)CH$_2$}$_2$][30] and 359 ppm for **8**, see below), so it is likely that at low concentrations, thf coordination to the monomer gives rise to the resonance at 224 ppm, with the dimer at 54 ppm. At high concentrations, the dimer predominates.

Single crystals of **5** and **6** suitable for X-ray diffraction were grown from saturated thf solution and a thf solution layered with petroleum ether respectively. Their molecular structures were determined and revealed dimeric species with dative N–Sn bonds from the nitrogen attached to the C$_2$H$_4$-fluorenyl tether; the least sterically congested N atom (Fig. 4).

The structure of **5** featured a neutral fluorenyl ring with tetrahedral C1 and a H atom attached, whereas **6** is doubly deprotonated causing C1 to become trigonal planar. Compared to **5**, the C–C bond lengths in the aromatic 5-membered rings in **6** have decreased for the bonds to C1 (from an average of 1.522 Å in **5** to an average of 1.416 Å in **6**) and conversely lengthened

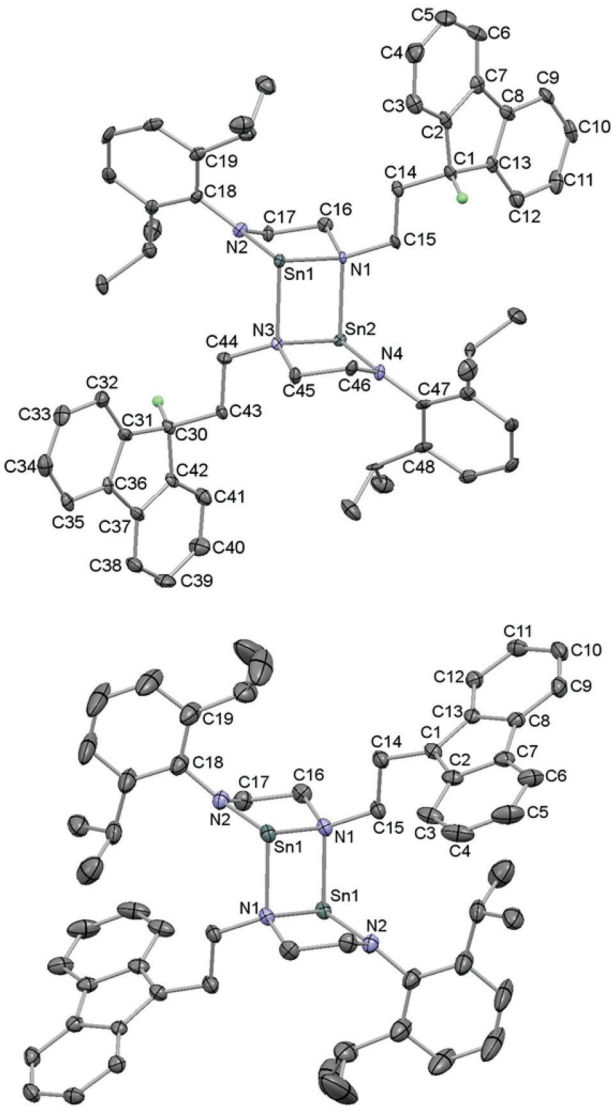

Fig. 4 Thermal ellipsoid plots (50% probability) of the molecular structures of **5** (top) and the dianionic portion of **6** (bottom). All H atoms, except the fluorenyl 9-H, and the [Li(thf)$_4$]$^+$ cations have been omitted for clarity. Symmetry operator used to generate symmetry generated atoms in **6**: $-x + 1$, $-y + 1$, $-z + 1$.

Table 1 Selected bond distances (Å) and bond angles (°) for compounds **5** and **6**

5	Sn1–N1	2.223(5)	Sn2–N3	2.229(5)
	Sn1–N2	2.083(5)	Sn2–N4	2.087(6)
	Sn1–N3	2.277(5)	Sn2–N1	2.278(5)
	C1–C2	1.517(10)	C30–C31	1.532(10)
	C1–C13	1.516(9)	C30–C42	1.524(9)
	C2–C7	1.403(10)	C31–C36	1.395(9)
	C7–C8	1.467(10)	C36–C37	1.459(9)
	C8–C13	1.402(10)	C37–C42	1.409(10)
	N1–Sn1–N2	79.7(2)	N3–Sn2–N4	79.7(2)
	Σ (angles at N1)	337.4	Σ (angles at N3)	337.9
	Σ (angles at N2)	358.2	Σ (angles at N4)	359.0
	Σ (angles at C1)	325.9	Σ (angles at C30)	327.2
6	Sn1–N1	2.227(2)	C1–C2	1.415(3)
	Sn1–N2	2.074(2)	C1–C13	1.416(3)
	Sn1–N1[a]	2.283(2)	C2–C7	1.443(3)
	Σ (angles at N1)	335.5	C7–C8	1.430(3)
	Σ (angles at N2)	357.0	C8–C13	1.448(3)
			Σ (angles at C1)	360

[a] Symmetry generated atom.

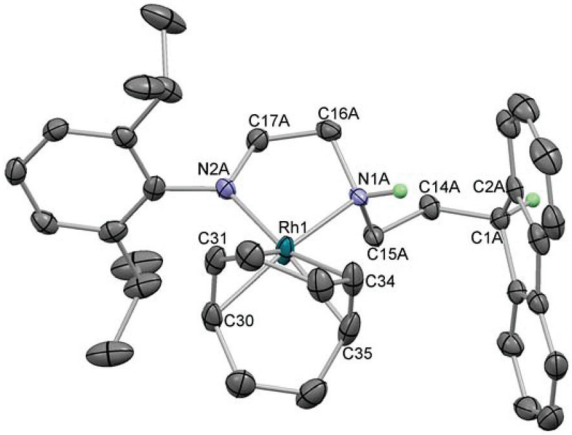

Fig. 5 Thermal ellipsoid plot of the molecular structure of **7** (50% probability). All H atoms, except the fluorenyl 9-H and the N–H, have been omitted for clarity. Only the major positions of the disordered fluorene group and ligand backbone are shown (ratio of disordered components 0.63 : 0.37). Selected bond distances (Å) and angles (°) for **7**: Rh1–C30 2.129(2), Rh1–C31 2.114 (2), Rh1–C34 2.113(2), Rh1–C35 2.107(2), Rh1–N1A 2.168(6), Rh1–N2A 2.008(9), Rh1–N1B 2.117(11), Rh1–N2B 2.003(15); Σ (angles at C1A) 332.1, Σ (angles at C1B) 333.3, Σ (angles at N1A) 327.3, Σ (angles at N1B) 328.0, Σ (angles at N2A), 359.9, Σ (angles at N2B) 356.8.

for the benzene-fused C–C bonds from an average of 1.402 Å in **5** (C2–C7, C8–C13, C30–C42 and C31–C36) to an average of 1.446 Å in **6** (C2–C7 and C8–C13). There are no significant interactions between the $[Li(thf)_4]^+$ cations and fluorenide rings. Other 'naked', uncoordinated fluorenide anions are known with the lithium cations coordinated to four molecules of thf,[64] two molecules of ethylenediamine[65] or two diglyme solvent molecules.[66] Bond lengths and angles for **5** and **6** are given in Table 1 and show the shortest Sn–N distances to the planar, three coordinate N(Dipp) atoms (2.074(2)–2.087(6) Å), intermediate distances to the other N atoms in the chelates (2.223(5)–2.229(5) Å) and the longest distances in the dative interactions (2.277(5)–2.283(2) Å) which feature pyramidalised N atoms. These features have been observed previously such as in a dimeric, mesityl-substituted saturated NHSn.[30]

Rhodium coordination chemistry

Two routes were investigated for the formation of bimetallic Sn–Rh compounds: reaction of the lithiated ligand precursor **2** with Rh salts followed by transamination with SnN''_2, or reaction of dianionic NHSn **6** with Rh salts. The reaction of monolithiated **2** with $[\{Rh(cod)(\mu\text{-}Cl)\}_2]$ in Et_2O produced an initially dark red solution that turned pale yellow after a few minutes. ^{1}H NMR spectroscopy revealed a highly asymmetric structure with four doublets and two septets for the Dipp group indicating hindered rotation around the N–Ar bond, resonances integrating to one for the signals arising from the methylene groups, and a Fl 9-H triplet still evident. Crystallisation from slow diffusion of petroleum ether into a Et_2O solution of **7** gave crystals suitable for X-ray diffraction, and the molecular structure of **7** revealed a square planar Rh(I) centre coordinated to cyclooctadiene (cod) and the ligand *via* one amide and one amine donor (Fig. 5). Anionic amide donors to Rh are relatively uncommon,[67] but Rh–Fl chemistry is also not extensive. A phosphine-tethered η^5-Fl Rh compound has been characterised by NMR spectroscopy[68] and only two η^5-Fl Rh compounds have been crystallographically characterised[69] (see below for the second example), along with a handful of η^1 examples.[70,71] This sparsity, compared to the wealth of Rh–Cp compounds, probably represents the underlying lower stability of TM-Fl binding,[72] and compound **7** is evidently more energetically stable as a square planar complex with a chelate ring composed of one amine and one amide donor. In the formation of **7**, however, the dark red colour initially observed suggests that a fluorenide intermediate is transiently formed which then rapidly isomerises to the more stable amide complex. A similar transformation has been observed for a mixed imidazolium–fluorenide ligand that displayed fast isomerization to its NHC–fluorenyl form upon coordination to Rh.[71]

Compound **7** was found to be unsuitable for the formation of the desired tethered NHSn complexes as addition of SnN''_2 to this species led to no reaction at room temperature after several days, whereas heating resulted in decomposition. Therefore, the alternative route in which dianionic NHSn **6** was reacted with $[\{Rh(cod)(\mu\text{-}Cl)\}_2]$ was subsequently attempted. NMR analysis of the crude reaction mixture in C_6D_6 after short reaction times revealed the presence of two new species. The ^{119}Sn NMR spectrum presented two signals: a singlet at 359 ppm and a doublet at 136 ppm with $^1J_{SnRh}$ = 630 Hz that disappeared after 2 hours at room temperature. The latter compound is tentatively assigned as a species where the stannylene is interacting with the Rh(cod) fragment and the fluorenide, if bound to the metal, is coordinated with low hapticity. Compound **8**, with a singlet resonance observed by ^{119}Sn NMR spectroscopy and no coupling to rhodium, is the

major product after loss of the initial species at 136 ppm, and multinuclear NMR spectroscopy was used to characterise it in solution. The ^{119}Sn chemical shift was very similar to other 2-coordinate NHSns such as [Sn{N(Dipp)CH$_2$}$_2$] (366 ppm) which suggested that the final product was a fluorenyl–Rh(cod) complex with an uncoordinated stannylene arm (**8**). This species is relatively unstable, decomposing over the course of several days in solution at room temperature. In order to confirm the assignment of this heterobimetallic complex, crystallisation of the compound was achieved by layering filtered benzene solutions with petroleum ether, and yellow crystals suitable for X-ray diffraction were grown. Although the data were of poor quality, connectivity was unambiguously established. The compound shows a dimeric structure through dative Sn–N bonds with Rh(cod) moieties bound η^5 to each of the fluorenyl 5-membered rings (**9**, Fig. 6). This is only the second crystallographically-characterised Rh complex to feature an η^5 fluorenyl interaction.[69] The solid-state structure of this compound is dimeric, in contrast to the proposed species in solution which in C_6D_6 revealed one sharp singlet resonance at 359 ppm by ^{119}Sn NMR spectroscopy indicating a monomeric, unsolvated species in non-coordinating solvents. However, the very broad ^{119}Sn NMR resonance at *ca.* 218 ppm in d^8-thf suggests an interconversion between solvated and unsolvated species in this solvent.

These observations suggest that the choice of the ancillary ligand at the Rh centre is likely to be crucial, and that cod is not labile enough for coordination of the pendent NHSn arm. Further reactions utilising different co-ligands on Rh to generate NHSn binding and control subsequent reactivity are currently underway.

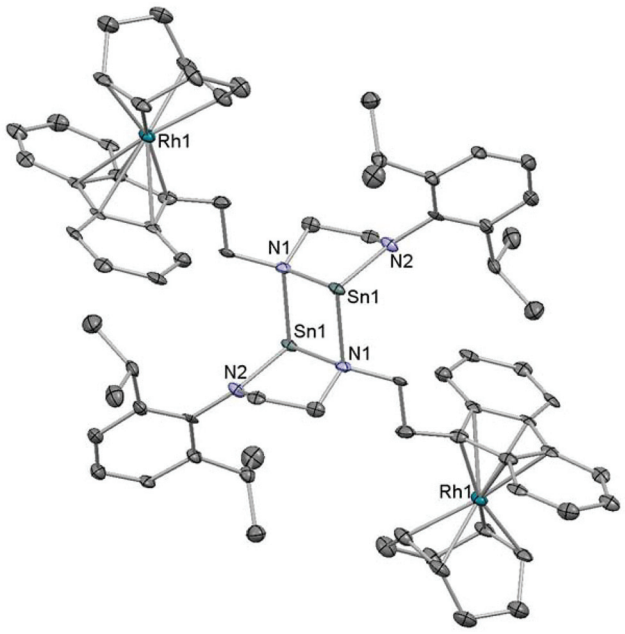

Fig. 6 Thermal ellipsoid plot of the molecular structure of **9** (50% probability). All H atoms have been omitted for clarity. Symmetry operator used to generate symmetry generated atoms: $-x + 1$, $-y + 1$, $-z + 1$.

Experimental

General synthetic details

Experiments were performed under dry, oxygen free N_2 using standard Schlenk-line and glovebox techniques except in the synthesis of the diamine ligand precursors which were performed in the open laboratory. Petroleum ether (40–60) and diethyl ether were distilled under nitrogen from sodium wire and sodium wire/benzophenone respectively, freeze–pump–thaw degassed and stored over activated 4 Å molecular sieves. Toluene, tetrahydrofuran (thf) and CH_2Cl_2 (DCM) were dried using a commercial solvent purification system and degassed. Deuterated solvents were dried over molten potassium (C_6D_6 and C_7D_8), CaH_2 ($CDCl_3$) or activated 4 Å molecular sieves (d^8-thf) and were degassed before use. ^{1}H and ^{13}C NMR spectra were recorded on Bruker AVIII400 (400 MHz), AVI400 (400 MHz) or AVIII300 (300 MHz) spectrometers referenced to internal solvent resonances, ^{119}Sn and ^{7}Li NMR spectra were recorded on a Bruker AVIII400 spectrometer referenced to external samples of $SnMe_4$ (δ 0 ppm) and LiCl/D_2O (δ 0 ppm) respectively. ESI mass spectrometry was carried out using a Bruker MicroToF 2 mass spectrometer at the University of Edinburgh. Elemental analyses were conducted using an Exeter CE-440 elemental analyser at Heriot-Watt University or by Mr Stephen Boyer at London Metropolitan University for air-sensitive samples. Despite repeated attempts, satisfactory elemental analyses could not be obtained for the lithium salts **2**, **3** and **4**. Multinuclear NMR spectra are provided in the ESI as confirmation of their purity. Column chromatography was performed using silica gel (60 Å, particle size 35–70 μm). The starting materials SnN″$_2$ {N″ = N(SiMe$_3$)$_2$},[24] DippN(H)$C_2H_4NH_2$ (Dipp = 2,6-*i*-Pr$_2$C$_6$H$_3$),[73] and FlC_2H_4Br[74,75] were prepared by literature methods. The synthesis of ^{t}BuN(H)-$C_2H_4NH_2$ was adapted from the literature[76] (see ESI† for details). All other reagents were supplied commercially.

(9H-C$_{13}$H$_9$)C$_2$H$_4$N(H)C$_2$H$_4$N(H)Dipp (1a). FlC_2H_4Br (0.5 g, 1.83 mmol) and DippN(H)$C_2H_4NH_2$ (2 g, 9.08 mmol, 5 eq.) were heated at 115 °C for 16 hours in a stoppered flask. KOH (110 mg, 2.01 mmol, 1.1 eq.) was added to the resulting brown oil and the mixture was distilled at 100 °C, 7×10^{-2} mbar to recover the excess of diamine. The remaining brown paste was extracted with diethyl ether (3×3 cm^3) and the volatiles removed under reduced pressure yielding a brown oil that was purified by column chromatography (CH_2Cl_2 initially to elute the spirocyclopropane derivative followed by ethyl acetate) yielding **1a** as an off-white solid (640 mg, 1.55 mmol, 85%) which can be recrystallized from *n*-hexane. Colourless crystals suitable for X-ray analysis were obtained from concentrated *n*-hexane solutions, the $P\bar{1}$ polymorph at −25 °C and the $P2_1/n$ polymorph from slow evaporation at room temperature. ^{1}H-NMR (400 MHz, 25 °C, $CDCl_3$): δ = 7.78 (d, $^3J_{HH}$ = 7.0 Hz, 2H, Ar$_{Fl}$ H), 7.56 (dd, $^3J_{HH}$ = 7.5 Hz, $^4J_{HH}$ = 0.7 Hz, 2H, Ar$_{Fl}$ H),

7.40 (m, 2H, Ar_{Fl} H), 7.33 (m, 2H, Ar_{Fl} H), 7.11–7.02 (m, 3H, Dipp Ar H), 4.13 (t, $^3J_{HH}$ = 5.7 Hz, 1H, 9*H*-fluorene), 3.28 (sept, $^3J_{HH}$ = 6.9 Hz, 2H, Dipp CH), 2.89 (m, 2H, CH_2), 2.77 (m, 2H, CH_2), 2.57 (m, 2H, CH_2), 2.30 (m, 2H, CH_2), 1.22 (d, $^3J_{HH}$ = 6.7 Hz, 12H, Dipp CH_3); ^{13}C-NMR (100 MHz, 25 °C, $CDCl_3$): δ = 147.2 (Ar_{Fl} C_q), 143.6 (Dipp-*ipso*), 142.5 (Dipp-*ortho*), 141.1 (Ar_{Fl} C_q), 127.2 (Ar_{Fl} CH), 127.1 (Ar_{Fl} CH), 124.4 (Ar_{Fl} CH), 123.7 (Dipp-CH), 123.6 (Dipp-CH), 120.0 (Ar_{Fl} CH), 51.4 (CH_2), 50.0 (CH_2), 46.4 (9*C* fluorene), 45.9 (CH_2), 33.5 (CH_2), 27.7 (CH ^{i}Pr), 24.4 (CH_3 ^{i}Pr); elemental analysis calcd (%) for $C_{29}H_{36}N_2$: C 84.42, H 8.79, N 6.79; found: C 84.07, H 8.80, N 6.69.

Li{($C_{13}H_8$)C_2H_4N(H)C_2H_4N(H)Dipp} (2). *n*-BuLi (0.18 cm^3, 1.52 M in *n*-hexane, 0.27 mmol) was added to a solution of **1a** (102 mg, 0.25 mmol) in dry toluene (3.0 cm^3) at 0 °C forming a light orange solution. After the solution was allowed to warm to room temperature, it was stirred for 30 min. The solvent was removed under reduced pressure and the residue was washed with petroleum ether (2.0 cm^3) yielding an orange solid (55 mg, 0.13 mmol, 52% yield). The reaction proceeded cleanly to completion by ^{1}H NMR spectroscopy, but isolating the product in a glovebox leads to a lower yield. ^{1}H-NMR (400 MHz, 60 °C, d^8-tol): δ = 8.08 (d, $^3J_{HH}$ = 7.8 Hz, 2H, Ar_{Fl} H), 7.58 (d, $^3J_{HH}$ = 7.8 Hz, 2H, Ar_{Fl} H), 7.32 (t, $^3J_{HH}$ = 7.3, 2H, Ar_{Fl} H), 6.88–6.82 (m, 3H, Dipp + Ar_{Fl} H), 6.74 (m, 2H, Dipp Ar H), 3.35 (t, $^3J_{HH}$ = 6.6 Hz, 2H, CH_2), 2.82 (br, 2H), 2.07–1.88 (m, 4H), 1.83 (br, 1H), 1.38–1.21 (m, 2H), 0.81 (br, 12 H, Dipp CH_3), 0.14 (br, 1H). ^{7}Li-NMR (155.4 MHz, 60 °C, d_8-tol): δ = −5.69. (See ESI† for ^{1}H, ^{13}C and ^{7}Li NMR data for the THF adduct and for spectra of **2** at room temperature).

Li_2{($C_{13}H_8$)C_2H_4N(H)C_2H_4NDipp} (3). *n*-BuLi (0.07 mL, 1.52 M in hexane, 0.10 mmol) was added to a solution of **1a** (20 mg, 0.05 mmol) in benzene (0.5 cm^3) at 0 °C, forming a deep orange solution. After removal of volatiles under reduced pressure, the product was analysed by NMR spectroscopy upon addition of C_6D_6 and the reaction was found to have proceeded cleanly to completion. ^{1}H-NMR (400 MHz, 25 °C, C_6D_6): δ = 8.20 (d, $^3J_{HH}$ = 7.9 Hz, 1H, Ar_{Fl} H), 7.69 (d, $^3J_{HH}$ = 8.5 Hz, 1H, Ar_{Fl} H), 7.65 (d, $^3J_{HH}$ = 7.6 Hz, 1H, Ar_{Fl} H), 7.55 (m, 1H, Ar_{Fl} H), 7.50 (d, $^3J_{HH}$ = 8.9 Hz, 1H, Ar_{Fl} H), 7.19 (t, $^3J_{HH}$ = 7.3 Hz, 1H, Ar_{Fl} H), 6.96–6.85 (m, 4H, Ar_{Fl} H + Dipp Ar H), 6.23 (m, 1H, Ar_{Fl} H), 3.33 (m, 1H, CH_2), 3.17 (m, 1H, CH_2), 2.96 (m, 1H, CH_2), 2.88 (m, 1H, CH_2), 2.56 (m, 1H, CH_2), 2.20 (m, 1H, CH_2), 2.06 (br s, 2H, Dipp CH), 1.93 (m, 2H, CH_2), 0.91 (d, $^3J_{HH}$ = 7.0 Hz, 6H, Dipp CH_3), 0.86 (br s, 6H, Dipp CH_3), 0.16 (m, 1H, DippN*H*); ^{13}C-NMR (100 MHz, 25 °C, C_6D_6): δ = 155.4 (Dipp-*ipso*), 144.6 (Dipp-*ortho*), 132.9 (Ar_{Fl} C_q), 130.5 (Ar_{Fl} C_q), 124.4 (Ar_{Fl} CH), 123.7 (Dipp CH), 122.0 (Ar_{Fl} CH), 121.2 (Dipp CH), 120.8 (Ar_{Fl} C_q), 120.2 (Ar_{Fl} CH), 118.5 (Ar_{Fl} C_q), 117.8, 116.2, 115.2, 114.7, 105.6 (collection of Ar_{Fl} CH), 90.5 (9*C* fluorene), 56.4 (CH_2), 49.5 (CH_2), 45.5 (CH_2), 28.1 (CH ^{i}Pr), 24.5 (CH_3 ^{i}Pr), 23.5 (CH_2); ^{7}Li-NMR (155.4 MHz, 25 °C, C_6D_6): δ = −2.53, −5.69.

Li_3{($C_{13}H_8$)C_2H_4N(H)C_2H_4NDipp} (4). *n*-BuLi (0.10 mL, 1.52 M in hexane, 0.15 mmol) was added to a solution of **1a** (20 mg, 0.05 mmol) in benzene at room temperature forming a red oily precipitate. The solvent was removed under reduced pressure and subsequent addition of d_8-THF revealed the formation of **4** in a reaction which had proceeded cleanly to completion. ^{1}H-NMR (400 MHz, 25 °C, d_8-THF): δ = 7.90 (d, $^3J_{HH}$ = 7.6 Hz, 2H, Ar_{Fl} H), 7.50 (d, $^3J_{HH}$ = 7.9 Hz, 2H, Ar_{Fl} H), 6.83 (t, $^3J_{HH}$ = 7.2 Hz, 2H, Ar_{Fl} H), 6.47 (d, $^3J_{HH}$ = 7.3 Hz, 2H, Dipp Ar H), 6.41 (t, $^3J_{HH}$ = 7.0 Hz, 2H, Ar_{Fl} H), 5.79 (br m, 1H, Dipp Ar H), 3.59 (br m, 2H, CH_2), 3.42–3.30 (m, 6H, Dipp CH + CH_2), 3.11 (br m, 2H, CH_2), 1.03 (d, $^3J_{HH}$ = 6.7 Hz, 12H, Dipp CH_3); ^{13}C-NMR (100 MHz, 25 °C, d_8-THF): δ = 161.8 (Dipp *ipso*), 136.5 (Ar_{Fl} C_q), 135.8 (Dipp *ortho*), 123.2 (Ar_{Fl} C_q), 127.7 (Dipp *meta* CH), 119.8 (Ar_{Fl} CH), 119.3 (Ar_{Fl} CH), 115.1 (Ar_{Fl} CH), 108.7 (Ar_{Fl} CH), 107.5 (Dipp *para* CH), 92.3 (9*C* fluorene), 65.4 (CH_2), 61.8 (CH_2), 59.5 (CH_2), 31.4 (CH_2), 28.8 (CH ^{i}Pr), 25.0 (CH_3 ^{i}Pr). ^{7}Li-NMR (155.4 MHz, 25 °C, C_6D_6): δ = 0.14.

[{Sn(9H-$C_{13}H_9$)$C_2H_4NC_2H_4$NDipp}$_2$] (5). A solution of $Sn[N(SiMe_3)_2]_2$ (266 mg, 0.60 mmol) in thf (1 cm^3) was added to a solution of **1a** (250 mg, 0.60 mmol) in thf (1 cm^3) in an ampoule equipped with a Youngs adaptor. After stirring overnight at room temperature, petroleum ether (3 cm^3) was added to the suspension to precipitate additional product. The solvent was removed by filtration and the remaining white solid was washed with an additional portion of petroleum ether (2 cm^3) then dried under reduced pressure to yield a colourless solid (284 mg, 0.25 mmol, 84% yield). ^{1}H-NMR (400 MHz, 25 °C, d_8-THF): δ = 7.79 (m, 2H, Ar_{Fl} H), 7.55 (d, $^3J_{HH}$ = 7.3 Hz, 1H, Ar_{Fl} H), 7.48 (d, $^3J_{HH}$ = 7.3 Hz, 1H, Ar_{Fl} H), 7.37–7.21 (m, 4H, Ar_{Fl} H), 7.01 (m, 2H, Dipp Ar H), 6.94 (m, 1H, Dipp Ar H), 3.98 (m, 2H, CH_2 + 9*H*-fluorene), 3.60 (br, 1H, Dipp CH), 3.49 (m, 1H, CH_2), 3.40 (m, 1H, Dipp CH), 3.28 (m, 1H, CH_2), 3.20 (m, 1H, CH_2), 3.14 (m, 2H, CH_2), 2.40 (m, 2H, CH_2), 1.20 (m, 3H, CH_3 ^{i}Pr), 1.11 (m, 3H, CH_3 ^{i}Pr), 0.96 (m, 6H, CH_3 ^{i}Pr); ^{13}C-NMR (100 MHz, 25 °C, d_8-THF): δ = 150.4 (C_q), 147.5 (C_q, ×2), 141.8 (C_q), 141.7 (C_q), 127.8 (CH), 127.6 (CH), 127.6 (CH), 125.1 (CH), 124.8 (CH), 124.1 (CH), 120.6 (CH), 61.3 (CH_2), 56.1 (CH_2), 49.8 (CH_2), 46.8 (9*C* fluorene), 34.1 (CH_2), 29.6 (CH ^{i}Pr), 29.0 (CH ^{i}Pr), 25.7 (CH_3 ^{i}Pr, ×2), 25.5 (CH_3 ^{i}Pr), 25.3 (CH_3 ^{i}Pr); ^{119}Sn (148 MHz, 25 °C, d_8-THF): δ = 67.3; elemental analysis calcd (%) for $C_{58}H_{68}N_4Sn_2$: C 65.81, H 6.47, N 5.29; found: C 65.76, H 6.43, N 5.18.

[Li(thf)$_4$]$_2$[{Sn($C_{13}H_8$)$C_2H_4NC_2H_4$NDipp}$_2$] (6). A solution of $LiN(SiMe_3)_2$ (44 mg, 0.26 mmol, 2 eq.) in thf (1.5 cm^3) was added to **5** (135 mg, 0.12 mmol, 1 eq.). The suspension was stirred at room temperature for 15 min yielding a deep red solution that was layered with petroleum ether (5 cm^3). Slow diffusion led to the formation of red crystals that were washed with petroleum ether (2 cm^3) to yield **6** (181 mg, 0.11 mmol, 93% yield). ^{1}H-NMR (400 MHz, 25 °C, d_8-THF): δ 7.87 (br, 2H, Ar_{Fl} H), 7.34 (br, 2H, Ar_{Fl} H), 6.93 (br, 1H, Ar_{Dipp} H), 6.84 (br, 4H, Ar_{Dipp} + Ar_{Fl} H), 6.39 (br, 2H, Ar_{Fl} H), 4.32 (br, 1H, CH_2), 3.96 (br, 1H, CH_2), 3.87–3.28 (br, 7H, CH_2 + CH ^{i}Pr), 3.05 (br, 1H, CH_2), 1.16 (br, 6H, CH_3 ^{i}Pr), 0.91 (br, 3H, CH_3 ^{i}Pr), 0.41 (br, 3H, CH_3 ^{i}Pr); ^{13}C-NMR (100 MHz, 25 °C, d_8-THF): δ 151.9 (C_q), 149.8 (C_q), 146.1 (C_q), 136.3 (C_q), 123.7, 123.3, 122.9 (CH Dipp, ×3), 119.1, 118.7, 113.9, 107.6 (CH Fl, ×4), 89.1 (9*C* fluorene), 61.9 (CH_2, ×2), 56.1 (CH_2), 52.8 (CH_2), 28.7, 27.2,

26.5; ^{119}Sn (148 MHz, 25 °C, 0.034 M in d_8-THF): δ = 52.9; ^{119}Sn (148 MHz, 25 °C, 0.003 M in d_8-THF): δ = 224.4 and 54.5; elemental analysis calcd (%) for $C_{90}H_{130}Li_2N_4O_8Sn_2$: C 65.62, H 7.95, N 3.40; found: C 65.49, H 7.82, N 3.28; m.p.: 106–111 °C (decomp. to green solid).

[Rh(cod){κ^2-(9H-$C_{13}H_9$)C_2H_4N(H)C_2H_4NDipp}] (7). A mixture of **1a** (75 mg, 0.18 mmol, 1 eq.) and LiN($SiMe_3$)$_2$ (32 mg, 0.19 mmol, 1 eq.) were dissolved in Et_2O (2 cm^3) and stirred at room temperature for 30 minutes, then [{Rh(cod)(μ-Cl)}$_2$] (45 mg, 0.09 mmol, 1 eq.) was added. After 1 hour at room temperature a yellow solution with pale precipitate had formed. This was filtered and the filtrate was concentrated to *ca.* 1 cm^3 and layered with petroleum ether (5 cm^3) to yield yellow crystals (82 mg, 0.13 mmol, 73% yield) after diffusion at room temperature. ^{1}H-NMR (400 MHz, 25 °C, C_6D_6): δ 7.61 (m, 2H, Ar_{Fl} H), 7.29–7.11 (m, 9H, Ar_{Fl} + Ar_{Dipp} H), 4.42 (sept, $^3J_{HH}$ = 6.9 Hz, 1H, CH ^{i}Pr), 4.00 (sept, $^3J_{HH}$ = 6.9 Hz, 1H, CH ^{i}Pr), 3.57 (t $^3J_{HH}$ = 5.2 Hz, 1H, 9*H*-Fl), 3.30 (m, 2H, CH cod), 3.07 (m, 1H, CH_2), 2.90 (m, 1H, CH_2), 2.74 (m, 1H, CH cod), 2.39–2.25 (m, 4H, CH cod, + CH_2) 2.22–1.99 (m, 5H, CH_2), 1.84–1.76 (m, 3H, CH_2), 1.68–1.49 (m, 2H, CH_2), 1.51 (d, $^3J_{HH}$ = 6.8 Hz, 3H, CH_3 ^{i}Pr), 1.46 (d, $^3J_{HH}$ = 7.1 Hz, 3H, CH_3 ^{i}Pr), 1.40 (m, 1H, CH_2), 1.42 (d, $^3J_{HH}$ = 6.8 Hz, 3H, CH_3 ^{i}Pr), 1.28 (d, $^3J_{HH}$ = 6.8 Hz, 3H, CH_3 ^{i}Pr) ^{13}C-NMR (100 MHz, 25 °C, C_6D_6): δ 153.4 (d, $^2J_{CRh}$ = 1.6 Hz, C_{ipso}), 147.0, 146.9 (C_q Dipp), 146.6, 145.8, 141.6, 141.3 (C_q Fl), 128.2, 128.0, 127.6, 126.9, 124.6, 124.2, 123.6, 123.3, 120.7, 120.5 (CH Dipp, ×3 + CH Fl, ×8), 80.4, 80.2 (d, $^1J_{CRh}$ = 14.0 Hz, CH cod), 69.7, 68.2 (d, $^1J_{CRh}$ = 11.8 Hz, CH cod), 58.5, 54.1, 46.8 (CH_2), 45.9 (9*C* Fl), 32.7, 31.7, 30.5, 30.2, 29.5 (CH_2), 27.8 (CH_3 ^{i}Pr), 27.2 (×2), 27.1 (CH ^{i}Pr + CH_3 ^{i}Pr), 24.5, 23.8 (CH_3 ^{i}Pr); elemental analysis calcd (%) for $C_{37}H_{47}N_2Rh$: C 71.37, H 7.61, N 4.50; found: C 71.27, H 7.59, N 4.43.

[Rh(cod){η^5-($C_{13}H_8$)C_2H_4N(Sn)(C_2H_4)NDipp}] (8). A solution of 18 mg (0.037 mmol) of [{Rh(cod)(μ-Cl)}$_2$] in 0.2 mL of dry d_8-thf was added to a solution of *in situ* prepared lithiated stannylene **6** (0.075 mmol) in 0.3 mL of dry d_8-thf. A dark red solution formed and complex **8** was the main species in solution after one hour at room temperature. ^{1}H-NMR (400 MHz, 25 °C, d_8-THF): δ 7.95 (d, $^3J_{HH}$ = 7.0 Hz, 1H, Ar H), 7.88 (d, $^3J_{HH}$ = 7.5 Hz, 1H, Ar H), 7.73 (d, $^3J_{HH}$ = 7.5 Hz, 1H, Ar H), 7.37 (d, $^3J_{HH}$ = 7.5 Hz, 1H, Ar H), 7.21–7.03 (m, 5H, Ar H), 7.00 (t, $^3J_{HH}$ = 7.3 Hz, 1H, Ar H), 6.94 (m, 1H, Ar H), 4.68 (m, 1H, CH cod), 4.16 (m, 1H, CH_2), 3.97–3.69 (m, 4H, mix of CH_2, CH ^{i}Pr and CH cod), 3.45–3.26 (m, 4H, mix of CH_2 and CH cod), 2.87 (m, 1H, CH_2), 2.74 (m, 1H, CH cod), 2.26 (m, 1H, CH_2), 2.02 (m, 1H, CH_2), 1.90–1.76 (m, 3H, CH_2), 1.46–1.35 (m, 2H, CH_2), 1.31–1.24 (m, 9H, CH_3), 1.14 (d, $^3J_{HH}$ = 6.7 Hz, 3H, CH_3), 1.07 (m, 2H, CH_2), 0.80 (m, 1H, CH_2); ^{13}C-NMR (100 MHz, 25 °C, d_8-THF): 155.8, 150.1, 147.1, 146.5, 145.7, 137.0, 136.8 (collection of C_q), 125.5, 124.7, 124.2, 123.6, 123.4, 123.1, 122.8, 122.3, 121.2, 120.6, 119.4 (collection of CH), 87.9 (br, CH cod), 83.2 (d, $^1J_{CRh}$ = 13.8 Hz, CH cod), 81.6 (CH_2), 65.5 (d, $^1J_{CRh}$ = 20.7 Hz, 9*C* Fl), 62.0, 61.9, 61.8 (2 CH_2 and 2 CH cod overlapping, assignment *via* {^{1}H,^{13}C}-correlation), 41.7 (CH_2), 36.0 (CH_2), 32.5 (CH_2), 28.8 (CH ^{i}Pr), 28.5 (CH ^{i}Pr), 27.0, 26.7, 26.5 (2 CH_2 + CH_3), the remaining 3 CH_3 signals are coincident with a THF resonance; ^{119}Sn (148 MHz, 25 °C, C_6D_6): δ = 359.

Crystallisation of [Rh(cod){η^5-($C_{13}H_8$)C_2H_4N(Sn)(C_2H_4)-NDipp}]$_2$ (9). [{Rh(cod)(μ-Cl)}$_2$] (14 mg, 0.08 mmol) was dissolved in benzene (0.7 cm^3) and added to a vial containing **6** (46.5 mg, 0.08 mmol) in a glovebox. After 3 hours, the dark red solution was filtered through glass fibre filter paper and then the solution was layered with petroleum ether (1 cm^3). After 3 days, yellow crystals of **9** with some dark precipitate was observed (4 mg, 0.002 mmol, 3%).

X-ray crystallographic studies

Single crystals of the samples were covered in inert oil and placed under the cold stream of a Bruker X8 APEXII four-circle diffractometer cooled to 100 K. Exposures were collected using Mo Kα radiation (λ = 0.71073). Indexing, data collection and absorption correction were performed using the APEXII suite of programs.[77] Structures were solved using direct or Patterson methods (SHELXS or SHELXT)[78] and refined by full-matrix least-squares (SHELXL)[78] interfaced with the programme OLEX2[79] (Table 2). Crystals of **5** were found to be non-merohedrally twinned. Accordingly, the data were detwinned and refined using an hklf5 refinement with two crystal domains of ratio 0.77 : 0.23. Crystals of **6** showed disorder in the Li(thf)$_4$ cations, which was modelled with the whole cation over two sites at 50% occupancy and with additional SIMU and DELU restraints. Crystals of **7** showed disorder in the ligand from N2 to the fluorene ring with modelling accomplished over two positions (ratio 0.63 : 0.37) using SAME constraints for the two positions. Crystals of **9** were found to be very poorly diffracting necessitating long collection times (120 seconds for each exposure) which still led to poor data quality. A number of reflections with poor f_{obs} *vs.* f_{calc} agreement were omitted to improve the data quality and the structure was modelled using the RIGU restraint as well as using ISOR on one C atom (C5 in the fluorenyl ring). However, the data still allowed connectivity within the structure to be definitively established. CCDC deposition numbers: 1424295–1424301, 1441450 and 1431076.

Conclusions

The synthesis of diamine-tethered fluorenyl ligand precursors was achieved after optimisation of the reaction conditions and using column chromatography to yield pure products. A more selective synthesis and easier purification was developed for the Dipp substituted compound, whereas the *t*-butyl substituted compounds were synthesised in lower yield and required more challenging purification. The deprotonation chemistry of FlC_2H_4N(H)C_2H_4N(H)Dipp revealed deprotonation at the most acidic site first forming a lithium–fluorenide contact ion pair. A second equivalent of *n*-BuLi deprotonated the more acidic DippN(H) next, keeping the Li–Fl interaction intact, but the trilithiate was only soluble in coordinating solvents which disrupted this structure. Transamination reactions with SnN″$_2$

Table 2 Crystallographic data for compounds **1a**, **2**, **5**–**7** and **9**

Identification code	**1a**	**2**	**5**	**6**	**7**	**9**
Empirical formula	$C_{29}H_{36}N_2$	$C_{44}H_{50}LiN_2$	$C_{62}H_{76}N_4OSn_2$	$C_{90}H_{130}Li_2N_4O_8Sn_2$	$C_{37}H_{47}N_2Rh$	$C_{74}H_{90}N_4Rh_2Sn_2$
Formula weight	412.60	628.89	1138.69	1647.23	622.67	1478.69
Temperature/K	100.0	100.0	100.0	100.0	100.0	100.0
Crystal system	Triclinic	Monoclinic	Monoclinic	Monoclinic	Triclinic	Monoclinic
Space group	$P\bar{1}$	$P2_1/n$	$P2_1/n$	$P2_1/c$	$P\bar{1}$	$P2_1/n$
a/Å	8.8412(7)	11.8817(17)	10.7998(4)	10.0025(4)	9.1513(4)	8.6300(8)
b/Å	10.2994(7)	13.807(2)	17.2527(7)	26.2852(11)	10.3881(4)	30.633(3)
c/Å	14.6904(11)	23.091(3)	29.5233(12)	16.4291(6)	18.6509(8)	11.9259(10)
α/°	90.460(3)	90	90	90	74.3931(17)	90
β/°	102.300(3)	97.086(7)	98.884(2)	97.9963(16)	87.7389(18)	101.213(5)
γ/°	111.703(3)	90	90	90	64.9866(17)	90
Volume/Å^3	1208.77(16)	3759.2(9)	5435.0(4)	4277.5(3)	1541.89(11)	3092.6(5)
Z	2	4	4	2	2	2
ρ_{calc} g cm^{-3}	1.134	1.111	1.392	1.279	1.341	1.588
μ/mm^{-1}	0.065	0.062	0.963	0.640	0.582	1.370
F(000)	448.0	1324.0	2336.0	1736.0	656.0	1504.0
Crystal size/mm^3	0.48 × 0.38 × 0.26	0.70 × 0.30 × 0.20	0.30 × 0.25 × 0.10	0.30 × 0.10 × 0.05	0.18 × 0.08 × 0.05	0.20 × 0.16 × 0.04
2Θ range for data collection/°	2.85 to 64.746	4.542 to 54.448	2.742 to 54.972	3.984 to 55.124	5.058 to 55.024	4.992 to 55.114
Index ranges	$-13 \le h \le 13$, $-15 \le k \le 15$, $-22 \le l \le 20$	$-15 \le h \le 15$, $-15 \le k \le 17$, $-28 \le l \le 29$	$-13 \le h \le 13$, $0 \le k \le 22$, $0 \le l \le 38$	$-11 \le h \le 13$, $-31 \le k \le 34$, $-21 \le l \le 20$	$-11 \le h \le 11$, $-12 \le k \le 13$, $-19 \le l \le 24$	$-10 \le h \le 11$, $-39 \le k \le 34$, $-12 \le l \le 15$
Reflections collected	32 628	52 995	13 312	71 212	31 630	30 195
Independent reflections	8568 [R_{int} = 0.0295, R_{sigma} = 0.0323]	8369 [R_{int} = 0.0456, R_{sigma} = 0.0372]	13 312 [R_{int} = N/A, R_{sigma} = 0.0677]	9794 [R_{int} = 0.0433, R_{sigma} = 0.0393]	7019 [R_{int} = 0.0277, R_{sigma} = 0.0297]	6896 [R_{int} = 0.1184, R_{sigma} = 0.1477]
Data/restraints/parameters	8568/0/290	8369/0/436	13 312/0/631	9794/35/671	7019/52/537	6896/444/374
GooF on F^2	1.025	1.011	1.260	1.052	1.064	1.110
Final R indexes [$I \ge 2\sigma(I)$]	R_1 = 0.0444, wR_2 = 0.1143	R_1 = 0.0422, wR_2 = 0.0956	R_1 = 0.0803, wR_2 = 0.1346	R_1 = 0.0344, wR_2 = 0.0626	R_1 = 0.0295, wR_2 = 0.0610	R_1 = 0.1046, wR_2 = 0.2380
Final R indexes [all data]	R_1 = 0.0600, wR_2 = 0.1237	R_1 = 0.0683, wR_2 = 0.1074	R_1 = 0.1021, wR_2 = 0.1411	R_1 = 0.0535, wR_2 = 0.0678	R_1 = 0.0394, wR_2 = 0.0645	R_1 = 0.1663, wR_2 = 0.2656
Largest diff. peak/hole/e Å^{-3}	0.43/−0.23	0.27/−0.20	1.05/−1.89	0.45/−0.37	0.45/−0.50	5.58/−2.02

generated a neutral, dimeric NHSn which was readily deprotonated with LiN″ to give a dimeric fluorenide-tethered NHSn which showed complex solution behaviour. Reactions with [{Rh(cod)(μ-Cl)}$_2$] led to a transiently stable Rh compound with fluorenyl and cod bound to Rh and leaving the NHSn uncoordinated. This compound was found to be a dimer in the solid state as was observed for all the tethered NHSns. Reactions of mono-lithiated **2** with [Rh(cod)(μ-Cl)}$_2$] did not lead to a Rh–fluorenyl complex with a pendent diamine arm, but instead led to isomerisation forming square planar Rh(cod) with a mixed amide/amine donor ligand.

Acknowledgements

The authors would like to thank Heriot-Watt University, The Royal Society (Research grant: RG130436) and the EPSRC (First grant: EP/M004767/1) for funding. Dr Mairi Haddow, for assistance with refining the crystal structure of **1b**, and Dr John Slattery, Dr Jason Lynam and Dr Pedro Aguiar, are also thanked for help with additional NMR experiments at the University of York.

Notes and references

1 C. Müller, D. Vos and P. Jutzi, *J. Organomet. Chem.*, 2000, **600**, 127.
2 P. McMorn and G. J. Hutchings, *Chem. Soc. Rev.*, 2004, **33**, 108.
3 H. Butenschön, *Chem. Rev.*, 2000, **100**, 1527.
4 U. Siemeling, *Chem. Rev.*, 2000, **100**, 1495.
5 S. T. Liddle, I. S. Edworthy and P. L. Arnold, *Chem. Soc. Rev.*, 2007, **36**, 1732.
6 P. Braunstein and F. Naud, *Angew. Chem., Int. Ed.*, 2001, **40**, 680.
7 R. Lindner, B. van den Bosch, M. Lutz, J. N. H. Reek and J. I. van der Vlugt, *Organometallics*, 2011, **30**, 499.
8 P. Jutzi and T. Redeker, *Eur. J. Inorg. Chem.*, 1998, 663.
9 J. R. Webb, S. A. Burgess, T. R. Cundari and T. B. Gunnoe, *Dalton Trans.*, 2013, **42**, 16646.

10 Z. R. Turner, R. Bellabarba, R. P. Tooze and P. L. Arnold, *J. Am. Chem. Soc.*, 2010, **132**, 4050.
11 A. L. McKnight and R. M. Waymouth, *Chem. Rev.*, 1998, **98**, 2587.
12 H. Braunschweig and F. M. Breitling, *Coord. Chem. Rev.*, 2006, **250**, 2691.
13 L. Lefort, T. W. Crane, M. D. Farwell, D. M. Baruch, J. A. Kaeuper, R. J. Lachicotte and W. D. Jones, *Organometallics*, 1998, **17**, 3889.
14 T. A. Mobley and R. G. Bergman, *J. Am. Chem. Soc.*, 1998, **120**, 3253.
15 S. P. Downing and A. A. Danopoulos, *Organometallics*, 2006, **25**, 1337.
16 S. P. Downing, S. C. Guadano, D. Pugh, A. A. Danopoulos, R. M. Bellabarba, M. Hanton, D. Smith and R. P. Tooze, *Organometallics*, 2007, **26**, 3762.
17 B. Royo and E. Peris, *Eur. J. Inorg. Chem.*, 2012, 1309.
18 A. P. da Costa, M. Sanau, E. Peris and B. Royo, *Dalton Trans.*, 2009, 6960.
19 A. P. da Costa, M. Viciano, M. Sanau, S. Merino, J. Tejeda, E. Peris and B. Royo, *Organometallics*, 2008, **27**, 1305.
20 L. Postigo, R. Lopes and B. Royo, *Dalton Trans.*, 2014, **43**, 853.
21 S. P. Downing, P. J. Pogorzelec, A. A. Danopoulos and D. J. Cole-Hamilton, *Eur. J. Inorg. Chem.*, 2009, 1816.
22 B. Wang, D. Cui and K. Lv, *Macromolecules*, 2008, **41**, 1983.
23 P. J. Davidson and M. F. Lappert, *J. Chem. Soc., Chem. Commun.*, 1973, 317.
24 M. J. S. Gynane, D. H. Harris, M. F. Lappert, P. P. Power, P. Riviere and M. Rivierebaudet, *J. Chem. Soc., Dalton Trans.*, 1977, 2004.
25 M. Asay, C. Jones and M. Driess, *Chem. Rev.*, 2011, **111**, 354.
26 B. Blom, D. Gallego and M. Driess, *Inorg. Chem. Front.*, 2014, **1**, 134.
27 L. Álvarez-Rodríguez, J. A. Cabeza, P. García-Álvarez and D. Polo, *Coord. Chem. Rev.*, 2015, **300**, 1.
28 T. Gans-Eichler, D. Gudat, K. Nattinen and M. Nieger, *Chem. – Eur. J.*, 2006, **12**, 1162.
29 T. Gans-Eichler, D. Gudat and M. Nieger, *Angew. Chem., Int. Ed.*, 2002, **41**, 1888.
30 S. M. Mansell, C. A. Russell and D. F. Wass, *Inorg. Chem.*, 2008, **47**, 11367.
31 A. V. Zabula and F. E. Hahn, *Eur. J. Inorg. Chem.*, 2008, 5165.
32 S. M. Mansell, R. H. Herber, I. Nowik, D. H. Ross, C. A. Russell and D. F. Wass, *Inorg. Chem.*, 2011, **50**, 2252.
33 A. V. Zabula, T. Pape, A. Hepp and F. E. Hahn, *Dalton Trans.*, 2008, 5886.
34 F. E. Hahn, A. V. Zabula, T. Pape, A. Hepp, R. Tonner, R. Haunschild and G. Frenking, *Chem. – Eur. J.*, 2008, **14**, 10716.
35 A. V. Zabula, T. Pape, A. Hepp and F. E. Hahn, *Organometallics*, 2008, **27**, 2756.
36 A. V. Zabula, T. Pape, A. Hepp, F. M. Schappacher, U. C. Rodewald, R. Poettgen and F. E. Hahn, *J. Am. Chem. Soc.*, 2008, **130**, 5648.
37 D. Gallego, S. Inoue, B. Blom and M. Driess, *Organometallics*, 2014, **33**, 6885.
38 F. E. Hahn, L. Wittenbecher, D. Le Van and A. V. Zabula, *Inorg. Chem.*, 2007, **46**, 7662.
39 J. Heinicke, A. Oprea, M. K. Kindermann, T. Karpati, L. Nyulászi and T. Veszprémi, *Chem. – Eur. J.*, 1998, **4**, 541.
40 A. V. Zabula, A. Y. Rogachev and R. West, *Chem. – Eur. J.*, 2014, **20**, 16652.
41 F. M. Mück, D. Kloß, J. A. Baus, C. Burschka and R. Tacke, *Chem. – Eur. J.*, 2014, **20**, 9620.
42 J. A. Cabeza, J. M. Fernández-Colinas, P. García-Álvarez, E. Pérez-Carreño and D. Polo, *Inorg. Chem.*, 2015, **54**, 4850.
43 K. M. Krebs, S. Freitag, H. Schubert, B. Gerke, R. Poettgen and L. Wesemann, *Chem. – Eur. J.*, 2015, **21**, 4628.
44 S. Krupski, C. S. T. Brinke, H. Koppetz, A. Hepp and F. E. Hahn, *Organometallics*, 2015, **34**, 2624.
45 R. J. Less, V. Naseri, M. McPartlin and D. S. Wright, *Chem. Commun.*, 2011, **47**, 6129.
46 J. A. Labinger and J. E. Bercaw, *Nature*, 2002, **417**, 507.
47 D. Das, S. S. Mohapatra and S. Roy, *Chem. Soc. Rev.*, 2015, **44**, 3666.
48 M. Flückiger and A. Togni, *Eur. J. Org. Chem.*, 2011, 4353.
49 A. R. Siedle, R. A. Newmark, B. F. Duerr and P. C. Leung, *J. Mol. Catal. A: Chem.*, 2004, **214**, 187.
50 P. Jutzi and U. Siemeling, *J. Organomet. Chem.*, 1995, **500**, 175.
51 R. D. Culp and A. H. Cowley, *Organometallics*, 1996, **15**, 5380.
52 9-Methylfluorene pK_a (DMSO): 22.3 whereas the pK_a of alkyl-arylamines and dialkylamines are higher *e.g.* HN-*i*-Pr_2: 36.
53 F. G. Bordwell and M. J. Bausch, *J. Am. Chem. Soc.*, 1983, **105**, 6188.
54 T. Kottke and D. Stalke, *Angew. Chem., Int. Ed. Engl.*, 1993, **32**, 580.
55 E. Kirillov, L. Toupet, C. W. Lehmann, A. Razavi and J. F. Carpentier, *Organometallics*, 2003, **22**, 4467.
56 H. V. Rasika Dias, Z. Wang and S. G. Bott, *J. Organomet. Chem.*, 1996, **508**, 91.
57 M. Konemann, G. Erker, R. Frohlich and E. U. Wurthwein, *J. Am. Chem. Soc.*, 1997, **119**, 11155.
58 E. Kirillov, J.-Y. Saillard and J.-F. Carpentier, *Coord. Chem. Rev.*, 2005, **249**, 1221.
59 D. Johnels, A. Andersson, A. Boman and U. Edlund, *Magn. Reson. Chem.*, 1996, **34**, 908.
60 M. Håkansson, C.-H. Ottosson, A. Boman and D. Johnels, *Organometallics*, 1998, **17**, 1208.
61 I. Fernandez, E. Martinez-Viviente, F. Breher and P. S. Pregosin, *Chem. – Eur. J.*, 2005, **11**, 1495.
62 L. Broeckaert, J. Turek, R. Olejník, A. Růžička, M. Biesemans, P. Geerlings, R. Willem and F. De Proft, *Organometallics*, 2013, **32**, 2121.
63 L. Wang, C. E. Kefalidis, T. Roisnel, S. Sinbandhit, L. Maron, J.-F. Carpentier and Y. Sarazin, *Organometallics*, 2015, **34**, 2139.

64 B. Becker, V. Enkelmann and K. Müllen, *Angew. Chem., Int. Ed. Engl.*, 1989, **28**, 458.
65 S. Buchholz, K. Harms, M. Marsch, W. Massa and G. Boche, *Angew. Chem., Int. Ed. Engl.*, 1989, **28**, 72.
66 S. Neander, J. Kornich and F. Olbrich, *J. Organomet. Chem.*, 2002, **656**, 89.
67 J. R. Fulton, A. W. Holland, D. J. Fox and R. G. Bergman, *Acc. Chem. Res.*, 2002, **35**, 44.
68 A. Doppiu, U. Englert and A. Salzer, *Chem. Commun.*, 2004, 2166.
69 S. I. Kallane, T. Braun, B. Braun and S. Mebs, *Dalton Trans.*, 2014, **43**, 6786.
70 C. Freund, N. Barros, H. Gornitzka, B. Martin-Vaca, L. Maron and D. Bourissou, *Organometallics*, 2006, **25**, 4927.
71 L. Benhamou, S. Bastin, N. Lugan, G. Lavigne and V. Cesar, *Dalton Trans.*, 2014, **43**, 4474.
72 H. G. Alt and E. Samuel, *Chem. Soc. Rev.*, 1998, **27**, 323.
73 C. Marshall, M. F. Ward and J. M. S. Skakle, *Synthesis*, 2006, 1040.
74 J. Kukral, P. Lehmus, M. Klinga, M. Leskelä and B. Rieger, *Eur. J. Inorg. Chem.*, 2002, 1349.
75 S. A. Miller and J. E. Bercaw, *Organometallics*, 2004, **23**, 1777.
76 I. K. Kormendy, *Acta Chim. Acad. Sci. Hung.*, 1958, **17**, 255.
77 *Bruker AXS APEX2*, version 2009-5, Bruker AXS Inc., Madison, Wisconsin, USA, 2009.
78 G. M. Sheldrick, *Acta Crystallogr., Sect. A: Fundam. Crystallogr.*, 2008, **64**, 112.
79 O. V. Dolomanov, L. J. Bourhis, R. J. Gildea, J. A. K. Howard and H. Puschmann, *J. Appl. Crystallogr.*, 2009, **42**, 339.